

Microsecond carrier lifetimes in InGaAsP quantum wells emitting at $\lambda=1.5 \mu\text{m}$

J. M. Smith^{a)} and G. S. Buller

Department of Physics, Heriot-Watt University, Riccarton, Edinburgh EH14 4AS, United Kingdom

D. Marshall^{b)} and A. Miller

Ultrafast Photonics Collaboration, School of Physics and Astronomy, University of St. Andrews, St. Andrews KY16 9SS, United Kingdom

C. C. Button^{c)}

EPSRC III-V Central Facility, University of Sheffield, Mappin Street, Sheffield S1 3JD, United Kingdom

(Received 4 September 2001; accepted for publication 14 January 2002)

Time-resolved photoluminescence measurements of an undoped InGaAsP multiple-quantum-well heterostructure at excess carrier densities between 10^{14} and 10^{16} cm^{-3} reveal unexpectedly long carrier lifetimes, in excess of $2 \mu\text{s}$. By fitting the appropriate rate equation parameters to our results, we establish that radiative recombination is the dominant relaxation process, and show that nonradiative recombination is much less pronounced than in similar quantum-well structures measured previously. © 2002 American Institute of Physics. [DOI: 10.1063/1.1459490]

InGaAsP heterostructures, with band gaps tunable in the wavelength range $1.1 \mu\text{m} < \lambda < 1.6 \mu\text{m}$, are of great interest in many areas of optoelectronics. In optical fiber-based telecommunications, their carrier recombination properties are important for determining their suitability for use in optoelectronics devices. For example, lasers and detectors require long lifetimes for high efficiency, and modulators require short lifetimes for high speed switching. It is desirable that nonradiative processes are weak in pure material, preferably to the degree whereby other recombination processes dominate, since nonradiative recombination rates can be increased by the deliberate introduction of defects. Long carrier lifetimes are also desirable in InGaAsP photovoltaics, for the development of high efficiency multijunction solar cells which make maximum use of the solar spectrum.

A large amount of work has been carried out investigating carrier relaxation in the InGaAsP material system at high injected carrier densities ($n > 10^{18} \text{ cm}^{-3}$),¹⁻⁴ typically revealing subnanosecond lifetimes which are attributable to Auger and radiative processes. In the intermediate range of carrier densities ($10^{16} \text{ cm}^{-3} < n < 10^{18} \text{ cm}^{-3}$), InGaAs quantum-well (QW) structures have tended to exhibit minority carrier lifetimes which are limited to a few tens of nanoseconds by nonradiative Shockley-Read-Hall (SRH) processes associated with barrier or interface defect states,⁵⁻⁷ while thicker layer InGaAsP double heterojunctions (DHs) have displayed radiative-dominated recombination.^{8,9} More recently, Ahrenkiel *et al.*¹⁰ have shown that the low density limit in which SRH processes dominate free carrier recombination can occur as low as $n \approx 10^{14} \text{ cm}^{-3}$ in undoped InGaAs/InP DHs, resulting in minority carrier lifetimes as long as $15 \mu\text{s}$.

In this letter, we report time-resolved photoluminescence (TRPL) measurements of an undoped InGaAsP multiple-QW (MQW) structure with a peak luminescence wavelength of 1525 nm , at injected carrier densities between 10^{14} and 10^{16} cm^{-3} . In previous studies of this sample,¹¹ transient grating experiments determined the intrawell ambipolar diffusion coefficient. Here, we find good agreement with the previous measurements, and observe carrier lifetimes in excess of $2 \mu\text{s}$, dominated by radiative recombination. These are the longest carrier lifetimes yet recorded for any undoped QW structure.

The sample was grown lattice matched onto an *n*-type InP substrate, by metalorganic vapor phase epitaxy. It is comprised of a MQW structure, with 60 periods of 10 nm thick $\text{In}_{0.57}\text{Ga}_{0.43}\text{As}_{0.93}\text{P}_{0.07}$ QWs and 7 nm thick $\text{In}_{0.87}\text{Ga}_{0.13}\text{As}_{0.29}\text{P}_{0.71}$ barriers, sandwiched between a 500 nm InP buffer and a 250 nm InP capping layer.

TRPL was carried out by gated-mode single photon counting with an InGaAs/InP single-photon avalanche diode (SPAD) cooled to 120 K . The apparatus is a modification of a time-correlated single-photon counting instrument developed recently.¹² Optical excitation was provided using a gain-switched distributed feedback laser emitting pulses of 3 ns duration and 13 pJ energy, at a wavelength of $1.3 \mu\text{m}$. For the measurements over time ranges $> 2 \mu\text{s}$, the time-resolved signal was obtained by a box-car method, stepping the delay of a short SPAD gate (from a Hewlett Packard HP81110A pulse generator) relative to the excitation pulse, and measuring the count rate with a Stanford Research SR400 photon counter. This latter arrangement has an overall temporal resolution of $\sim 50 \text{ ns}$.

The sample was mounted in a liquid nitrogen-cooled continuous flow cryostat, and its surface was imaged using a Hamamatsu C1000 infrared vidicon and a frame grabber. The optical excitation spot diameters were fitted to a Gaussian beam profile taking into account the nonlinear response of the vidicon. Luminescence from a sample area $10 \mu\text{m}$ in

^{a)}Electronic mail: J.M.Smith@hw.ac.uk

^{b)}Present address: Terahertz Photonics Ltd, Livingston EH54 7EJ, UK.

^{c)}Present address: Bookham Technology Caswell, Towcester NN12 8EQ, UK.

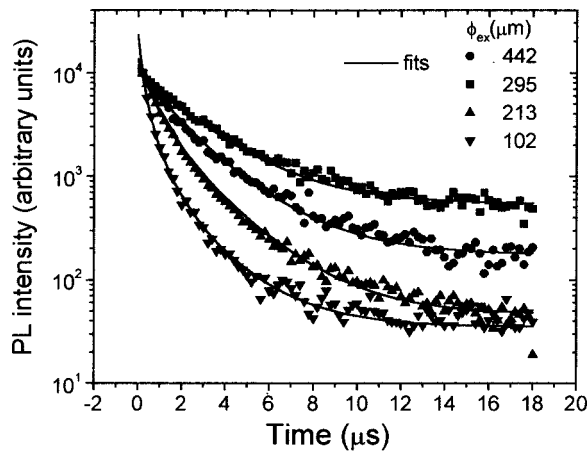


FIG. 1. TRPL for the InGaAsP MQW structure at 300 K, measured using different excitation spot diameters ϕ_{ex} and constant excitation energy per pulse. The ϕ_{ex} are $1/e^2$ values measured by fitting a Gaussian profile to the imaged excitation, and the area from which photoluminescence is collected is $\sim 10 \mu\text{m}$ diameter at the center of the excitation area in each case. Also shown are the theoretical decay curves corresponding to these ϕ_{ex} values, fitted using the rate Eq. (1).

diameter at the center of the excitation area was collected and focused into a 1550 nm single mode optical fiber coupled to the SPAD pigtail.

Figure 1 shows the room temperature TRPL decay of the heterostructure for excitation diameters, ϕ_{ex} , between 102 and 442 μm , the latter being the upper limit achievable using this apparatus. The peak sheet density of excess carriers, Δn_0 , excited by the 13 pJ optical pulses varies, as a result of this spot size adjustment, between $9.9 \times 10^9 \text{ cm}^{-2}$ and $5.3 \times 10^8 \text{ cm}^{-2}$, assuming an absorption coefficient of 10^4 cm^{-1} .

Also shown in Fig. 1 are the best fits of luminescence intensity versus time, calculated using the rate equation

$$\frac{\partial(\Delta n)}{\partial t} = -A\Delta n - \frac{2B}{w}(n_d + \Delta n)\Delta n - D\nabla^2(\Delta n), \quad (1)$$

where Δn is the sheet excess carrier density, A is the combined nonradiative recombination coefficient, B is the bulk radiative recombination coefficient, w is the quantum well width, n_d is the background donor concentration, and D is the ambipolar carrier diffusion coefficient. Implicit in the second term is the approximation that the electron-hole overlap integral normal to the layers is equal to unity, and that the average carrier spacing in this dimension is $w/2$. Auger recombination can safely be neglected for such weak excitation.²

The luminescence decays are not single exponentials, and vary considerably for the different excitation spot diameters. The time taken for the luminescence intensity to fall to $1/e$ of its initial value varies from $\sim 2.6 \mu\text{s}$ for the largest excitation diameter, ϕ_{ex} , to $\sim 0.6 \mu\text{s}$ for the smallest.

In the limit of large ϕ_{ex} , diffusion will be negligible and the excitation carrier density small. Monomolecular decay will dominate through linear radiative or nonradiative processes, which are independent of ϕ_{ex} . The significant difference between the data for the two largest ϕ_{ex} in Fig. 1 indicates that this limit has not been reached, and therefore, that diffusion and/or bimolecular radiative recombination are significant even at $\phi_{\text{ex}} = 442 \mu\text{m}$. Decreasing the excitation di-

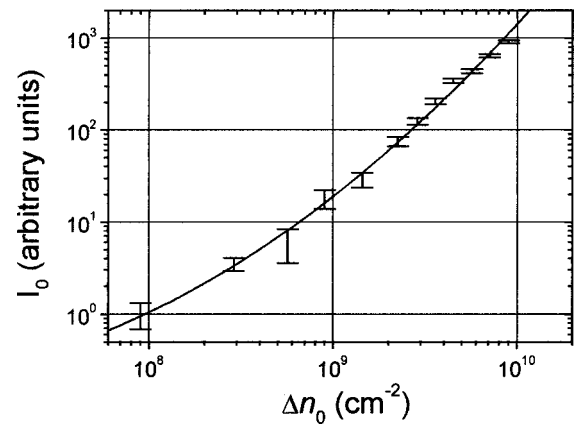


FIG. 2. Dependence of the (temporal) peak photoluminescence intensity I_0 on the injected carrier density Δn_0 . The best quadratic fit, suggested by the expression $I_0 \alpha (n_d + \Delta n_0)\Delta n_0$, is also shown. The ratio of the linear and quadratic coefficients of the fit lead to a value of the background doping concentration $n_d \approx 4 \times 10^9 \text{ cm}^{-2}$.

ameter increases the initial decay rate due to both an increased rate of diffusion of carriers out of the detection area, and the increasingly bimolecular nature of the radiative process with increasing Δn_0 . The fitted curves in Fig. 1 show excellent agreement throughout the range of ϕ_{ex} , corresponding to parameter values $B = 10^{-10} \text{ cm}^3 \text{ s}^{-1}$ and $D = 6 \text{ cm}^2 \text{ s}^{-1}$. The value of B is in good agreement with those found in Refs. 2 and 4, while D is close to the value of $7.2 \text{ cm}^2 \text{ s}^{-1}$ measured for this sample using the transient grating technique in Ref. 9. The combined linear recombination rate corresponding to these fits is

$$A + 2Bn_d/w = 2 \times 10^5 \text{ s}^{-1}. \quad (2)$$

Without measuring the background donor density n_d , Eq. (2) allows us to state with confidence only that $A < 2 \times 10^5 \text{ s}^{-1}$. We can estimate n_d from photoluminescence data, by measuring the dependence of the peak luminescence intensity I_0 on the initial injected carrier density Δn_0 (varied by attenuating the excitation pulses). This relationship is shown in Fig. 2, with $\phi_{\text{ex}} = 125 \mu\text{m}$ giving $\Delta n_0 = 1.2 \times 10^{10} \text{ cm}^{-2}$ for unattenuated excitation. Since only the initial luminescence intensity is measured, the form of the data is described by the second term of Eq. (1) (replacing Δn with Δn_0), and can thus be fitted by a quadratic expression. The fitted curve is included in Fig. 2, the quadratic coefficients of which indicate that $n_d \approx 4 \times 10^9 \text{ cm}^{-2}$. The error attributable to this value of the background carrier density is large due to the crudeness of the method employed, and it should only be taken as a guide. We note that with such a value for n_d the second term in Eq. (2) is comparable with the total linear recombination rate, and so the contribution from SRH recombination is likely to be considerably smaller than the upper limit derived earlier. Even with the largest excitation areas used, therefore, the recombination appears to be predominantly radiative.

Further evidence for this attribution is provided with the temperature dependence of the photoluminescence decays, show in Fig. 3. The decay lifetime is seen to decrease significantly between 300 and 100 K, and can be accounted for by including in our model a linear temperature dependence for B of $-3.5 \times 10^{-12} \text{ cm}^3 \text{ s}^{-1} \text{ K}^{-1}$. This value is in good

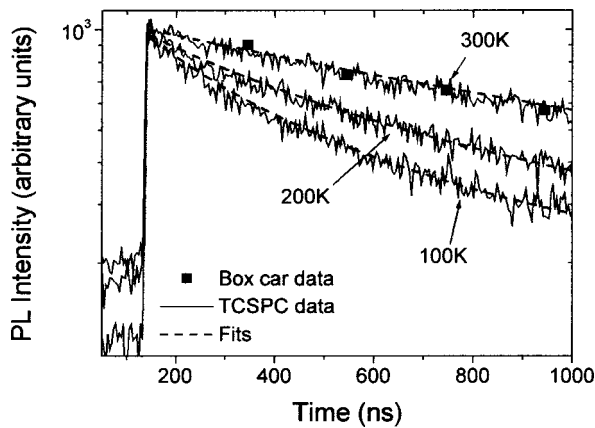


FIG. 3. Temperature dependence of the TRPL characteristics with a $300\ \mu\text{m}$ excitation spot diameter. The reduced lifetime at lowered temperature is consistent with a radiative recombination temperature coefficient of $dB/dT = -3.5 \times 10^{-12}\ \text{cm}^3\ \text{s}^{-1}\ \text{K}^{-1}$.

agreement with previous measurements of this parameter in $\text{In}_{0.53}\text{Ga}_{0.47}\text{As}$.¹³ Further spot-size dependent measurements at 100 K (not shown) indicate that the diffusion coefficient varies little with temperature, and we thus conclude that the reduced lifetime at low temperature results primarily from the increase in B .

There are two effects that we have not considered in the aforementioned analysis, which can serve to artificially increase the observed carrier lifetime. The first, photon recycling, has the effect of artificially increasing the diffusion coefficient by an additive term D_r and the radiative lifetime by a multiplicative factor φ .¹⁴ We estimate that $D_r \sim 0.1\ \text{cm}^2\ \text{s}^{-1}$, and $\varphi < 2$ in this MQW structure, so that the only significance to the analysis presented here would be that we have underestimated B by a factor of two at most. Note that our argument regarding SRH processes remains unaffected. The second effect, namely capture and re-emission of carriers by deep levels, can be rejected as a possible influence since its signature is a decay time constant that increases with reduced temperature, inconsistent with our observations.

The longest lifetime observed previously in a comparable structure is 60 ns by Fancey *et al.*,⁷ in an InGaAs/InGaAsP MQW. In that study, injected carrier densities of $\sim 10^{17}\ \text{cm}^{-3}$ were used, and so their measured lifetime is not far from the predicted radiative value, given by $(B\Delta n)^{-1}$, of ~ 100 ns. It may then be worth noting that the two structures exhibiting the longest lifetimes to date have incorporated quaternary barriers.

An interesting comparison can be made here with GaAs MQW structures, in which increased rates of monotonic re-

combination in narrower QWs implies the dominance of SRH recombination through centers either at the interfaces or in the barriers themselves. This SRH dominance does not appear to be the case in InGaAsP MQWs, although a study of the dependence of carrier lifetime on QW width has yet to be undertaken. The apparently lower SRH contribution in InGaAsP appears despite the fact that interfaces are thought to be rougher than in GaAs MQWs, a hypothesis borne out by comparison of hole diffusion coefficients in the two MQW systems.¹¹

We have used photon counting TRPL to measure carrier lifetimes in an InGaAsP MQW structure at excess carrier densities below $2 \times 10^{16}\ \text{cm}^{-3}$. Our results indicate that recombination is dominated by the radiative process, and an upper limit of $2 \times 10^5\ \text{s}^{-1}$ is placed on the nonradiative recombination coefficient. A lifetime of $2.6\ \mu\text{s}$ is observed when diffusion effects are minimized. With lifetimes in the microseconds regime, InGaAsP QW structures are extremely attractive for devices which require high radiative or photo-detection efficiency.

This work was supported by EPSRC (Refs. GR/L81895 and GR/L87125) and the European Commission Framework Five EQUIS project (Ref. IST-1999-11594). One of the authors (J.M.S.) would like to thank Mike Robertson and Paul Townsend of Corning Research Center, Ipswich, and Peter Blood of the University of Wales, Cardiff, for valuable discussions.

- ¹A. Miller, R. J. Manning, A. M. Fox, and J. H. Marsh, *Electron. Lett.* **20**, 601 (1984).
- ²E. Wintner and E. P. Ippen, *Appl. Phys. Lett.* **44**, 999 (1984).
- ³A. J. Taylor and J. M. Wiesenfeld, *Phys. Rev. B* **35**, 2321 (1987).
- ⁴A. M. Fox, R. J. Manning, and A. Miller, *J. Appl. Phys.* **65**, 4287 (1989).
- ⁵J. E. Ehrlich, D. T. Neilson, A. C. Walker, G. T. Kennedy, R. S. Grant, W. Sibbett, and M. Hopkinson, *Semicond. Sci. Technol.* **8**, 307 (1993).
- ⁶G. S. Buller, S. J. Fancey, J. S. Massa, A. C. Walker, S. Cova, and A. Lacaita, *Appl. Opt.* **35**, 916 (1996).
- ⁷S. J. Fancey, G. S. Buller, J. S. Massa, A. C. Walker, C. J. Maclean, A. McKee, A. C. Bryce, J. H. Marsh, and R. M. De La Rue, *J. Appl. Phys.* **79**, 9390 (1996).
- ⁸B. Sermage, H. J. Eichler, J. P. Heritage, R. J. Nelson, and N. K. Dutta, *Appl. Phys. Lett.* **42**, 259 (1983).
- ⁹C. H. Henry, B. F. Levine, R. A. Logan, and C. G. Bethea, *IEEE J. Quantum Electron.* **19**, 905 (1983).
- ¹⁰R. K. Ahrenkiel, R. Ellingson, S. Johnston, and M. Wanlass, *Appl. Phys. Lett.* **72**, 3470 (1998).
- ¹¹D. Marshall, A. Miller, and C. C. Button, *IEEE J. Quantum Electron.* **36**, 1013 (2000).
- ¹²J. M. Smith, P. A. Hiskett, and G. S. Buller, *Rev. Sci. Instrum.* **72**, 2325 (2001).
- ¹³E. Zielinski, H. Schweizer, K. Streubel, H. Eisele, and G. Weimann, *J. Appl. Phys.* **59**, 2196 (1986).
- ¹⁴J. W. Orton and P. Blood, *The Electrical Characterization of Semiconductors: Measurement of Minority Carrier Properties* (Academic, London, 1990).